Experimental study of the influence of thermal shock on mechanical properties of ceramic coating systems

Xiaona Li[1,*], Lihong Liang[1], Hua Wei[2], Yueguang Wei[1]

1 LNM, Institute of Mechanics, Chinese Academy of Sciences, Beijing, 100190, China
2 Institute of Metal Research, Chinese Academy of Sciences, Shenyang, 110016, China
* Corresponding author: lixiaona@lnm.imech.ac.cn

Abstract In this work, the change of Young's modulus, hardness, and bending strength of air plasma sprayed ceramic coating systems after different thermal shock was investigated by nanoindentation tests and three-point bending tests. The results of these tests show that the Young's modulus and hardness of nanostructured coatings and the bending strength of nanostructured coating-substrate systems fluctuate relatively slightly as the thermal shock temperature difference increases, while the Young's modulus and hardness of micro-structured coatings and the bending strength of micro-structured coating-substrate systems increase with the thermal shock temperature difference monotonously. Therefore, in the temperature range we studied, the mechanical properties of nanostructured coatings are less sensitive to the change of temperature and more stable than micro-structured coatings.

Keywords Ceramic coating systems, Thermal shock, Young's modulus, Bending strength

1. Introduction

Ceramic coatings are widely used because of their excellent thermal insulation, wear resistance and corrosion resistance [1, 2]. In the service condition of ceramic coatings, thermal shock frequently occurs. Therefore, in-depth understanding of the influence of thermal shock on mechanical properties of ceramic coating systems becomes significant. Some relevant studies on the effect of thermal shock on ceramic coatings have been reported. Bo Liang et al. [3] investigated the thermal shock resistances of nanostructured and conventional zirconia coatings deposited by atmospheric plasma spraying, and found that the nanostructured as-sprayed coating possessed better thermal shock resistance than the conventional coating. Chunxia Zhang et al. [4] studied the influence of thermal shock on insulation effect of nano-multilayer thermal barrier coatings, and acquired the change of thermal conductivity and impedance as function of thermal shock number. Moreover, some researches have shown that thermal shock could obviously affect the mechanical properties of Si-SiC coated C/C composites [5], fiber concrete [6], alumina–mullite–zirconia and alumina–mullite refractory materials[7]. However, there are few reports on the influence of thermal shock on mechanical properties of ceramic coating systems. Therefore, in this work, we studied the change of elastic modulus, hardness, and bending strength of air plasma sprayed ceramic coating systems by nanoindentation tests and three-point bending tests.

2. Experimental procedure

2.1. Specimen preparation

The ceramic coating system used in this study consists of YSZ (8 wt.% Y2O3 stabilized ZrO2) top coat prepared with atmospheric plasma spraying (APS), NiCrAlY (25.42wt.%Cr-5.1wt.%Al-0.48wt.%Y) bond coat prepared with high velocity oxygen fuel (HVOF) process and Ni-based superalloy substrate. The thickness of the top coat, bond coat and substrate is approximately 0.1 mm, 0.05 mm, and 1.35 mm separately. In our study, two kinds of ceramic coating layers were prepared---nano-scale and micro-scale microstructure, respectively.

2.2. Thermal shock tests

In the thermal shock tests, the specimens were heated with a rate of 20℃/min up to a preset temperature T_m (200 ℃, 500 ℃, and 800 ℃, respectively) and held at T_m for 20 min [8]. After that, the heated specimens were quickly placed into water at the ambient temperature (25 ℃) for quenching and maintained for 10 min [8]. Therefore, the thermal shock temperature difference ΔT is 175 ℃, 475 ℃, and 775 ℃, respectively. The mechanical property was then measured using nanoindentation and bending tests at room temperature.

2.3. Nanoindentation tests

The grinded and polished coatings were analyzed by nanoindentation tests in which the Agilent Technologies Nano Indenter G200 System was used. All indentations were done with a triangular pyramid Berkovich diamond indenter. The total number of measurement points for each sample was chosen to be 10. The indentation depth was 300 nm and the maximum load was 12 mN in the tests. The typical distance between two neighboring sites is above 50 μm aiming to avoid possible interference of measurements. During the indentation test，the indentation load and depth are measured by load cell and gap sensors.

2.4. Three-point bending tests

The three-point bending tests were done with a computer control electronic universal testing machine RG2000-5. The nominal dimensions of each specimen for the three-point bending test are 3 mm wide, 1.5 mm high and 15 mm long. The span length of the support is 10 mm. The tests were carried out under constant displacement rates 0.1 mm/min at the loading point. Consequently, we could acquire a series of load-displacement curves in the loading process.

3. Results and discussion

3.1. Influence of thermal shock on Young’s modulus and hardness of ceramic coatings

In the temperature range of 25-800℃，the results of these tests show that the Young’s modulus E and hardness H of nanostructured coatings fluctuate relatively slightly as the thermal shock

temperature difference ΔT increases, while that of micro-structured coatings increase with ΔT monotonously, as shown in Fig. 1. For the as-spayed coating, the Young's modulus of nanostructured coating $E_c = 161.2$ GPa and micro-structured coating $E_c = 101.4$ GPa, which are in good general agreement with former reports [9] [10] ; the hardness of nanostructured coating $H_c = 11.6$ GPa and micro-structured coating $H_c = 5.4$ GPa, which are close to some data in the literatures[2, 10] [11]. After the thermal shock test, we carefully examined the microstructure of specimens and found that the porosity of micro-structured coatings reduces relatively obviously with the increase of ΔT, while that of the nanostructured coatings changes a little. From the literature[12], for porous materials, the Young's modulus E can be described empirically by $E = E_0 \exp(-ap)$, where E_0 is the zero-porosity Young's modulus, p is the porosity, and a is an empirical constant. Therefore, the Young's modulus will increase as the porosity decreases, and our test results agree with this theoretical model.

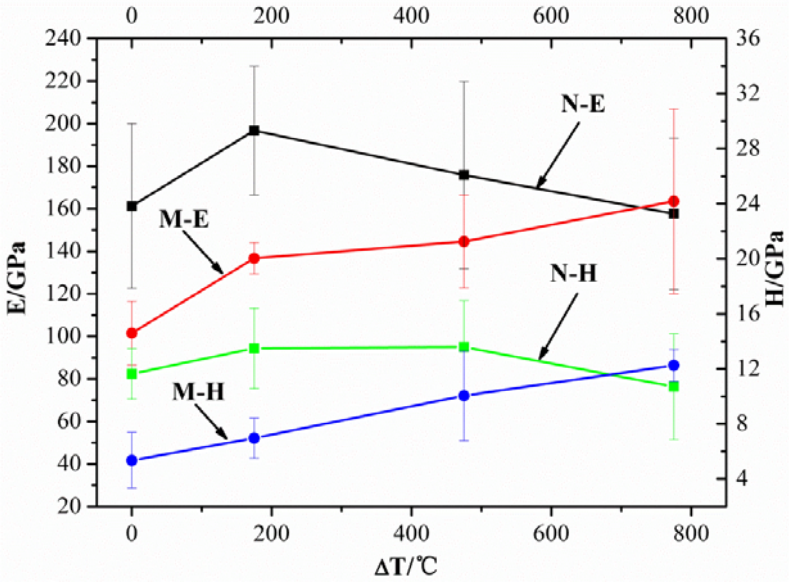

Figure 1. The change of Young's modulus and hardness of coatings with different thermal shock temperature difference ΔT (N-nanostructured coatings, M-micro-structured coatings).

3.2. Influence of thermal shock on bending strength of coating-substrate systems

One of the curves of the load F and loading point displacement w in our experiments is shown in Fig. 2. The maximum load was considered as the failure load and used to calculate the bending strength of coating-substrate systems.

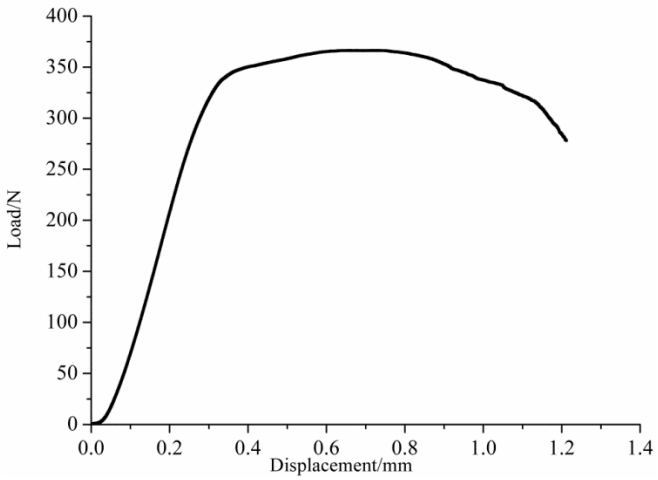

Figure 2. The load-displacement curve in three-point bending test.

During the three-point bending test, the largest normal stress at the failure load was considered to be the bending strength σ_b, which can be determined by Eq. (1) [13] as following:

$$\sigma_b = 0.8 \cdot (1 - \frac{4h}{3\pi l}) \cdot \frac{P_f l}{4} \cdot \frac{1}{M_0} \cdot \frac{E_c(h_c + \varsigma)}{E_s(h_s - \varsigma)} \qquad (1)$$

Where *l* and *h* are the span length of support and the height of specimens respectively, P_f is the failure load, h_c and h_s are the thickness of the coating and substrate respectively, E_c and E_s are the Young's modulus of coating and substrate respectively, ς is the distance between the neutral axis and the interface of the layered specimen, and M_0 is the resultant moment of the cross section. The values of ς and M_0 can be determined by $\varsigma = \frac{E_s h_s^2 - E_c h_c^2}{2(E_s h_s + E_c h_c)}$ and $M_0 = \frac{b}{3(\varsigma - h_s)}(h_s^3 - 3h_s^2\varsigma + 3h_s\varsigma^2) + \frac{E_c}{E_s}\frac{b}{3(\varsigma - h_s)}(h_c^3 + 3h_c^2\varsigma + 3h_c\varsigma^2)$, respectively, where *b* is the width of the specimen. The bending strength of all specimens obtained by Eq. (1) is presented in Fig. 3. It is worth mentioning that (1) the top coat and bond coat are considered as one layer, i.e. the coating, considering that Young's modulus of the bond coat is about 155 GPa [10, 14] which is close to that of the top coat, and the top coat and bond coat bind well according to our experimental observation, (2) the value of E_c is obtained from Fig. 2, and (3) the value of E_s is assumed constant and taken as 200 GPa [10] [15].

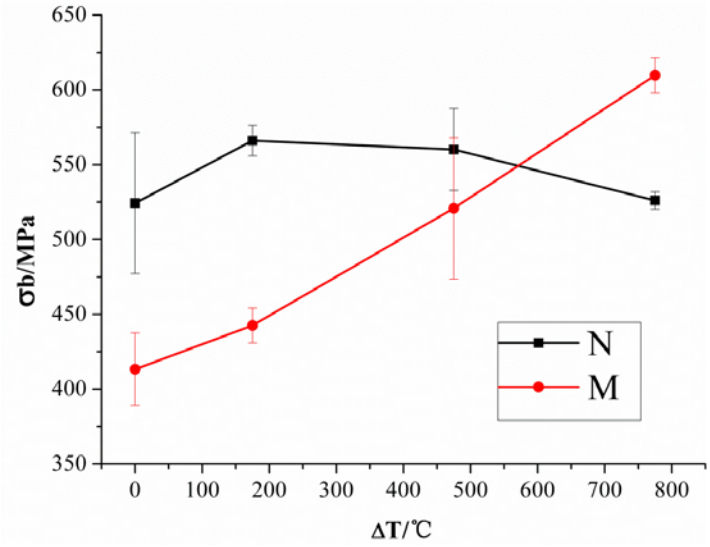

Figure 3. The change of bending strength of coating-substrate systems with different thermal shock temperature difference ΔT (N- nanostructured coatings, M- micro-structured coatings).

From Fig. 3, we can see that like the change of Young's modulus and hardness of coatings with different thermal shock temperature difference ΔT, the bending strength of nanostructured coating-substrate systems fluctuate relatively slightly as ΔT increases, while that of micro-structured coating-substrate systems increase monotonously with ΔT.

The bending strength of coating-substrate systems is determined by the strength of coating and substrate, and the interfacial bonding strength. In the temperature range of 25-800℃, the yield strength of the substrate is considered as constant[16]. Therefore, the main parameters are the strength of coating and the interfacial bonding strength. For porous materials, like the relationship between Young's modulus and porosity, the strength can be empirically described by $\sigma = \sigma_0 \exp(-kp)$ [17], where σ_0 is the zero-porosity strength, p is the porosity, and k is an empirical constant. Therefore, the strength will increase as the porosity decreases. Besides, according to our experimental observation, for micro-structured coating-substrate systems, the interfacial bonding strength decreases as the thermal shock temperature difference increases, while that of the nanostructured coating-substrate systems changes a little. Since the strength of coating-substrate systems is obviously influenced by the interfacial bonding strength, and weakening of interfaces helps to increase the bending strength of coating-substrate systems, [5] we can see that it is the combined effect of porosity of the coating and interfacial bonding strength of the coating-substrate that leads to the result of our tests.

4. Conclusions

In this work, the change of elastic modulus, hardness and bending strength of air plasma sprayed ceramic coating systems after different thermal shock was investigated by nanoindentation tests and three-point bending tests. The results of these tests show that (1) since the porosity of

micro-structured coatings reduces relatively obviously, while that of the nanostructured coatings changes a little with the increase of thermal shock temperature difference, the Young's modulus and hardness of nanostructured coatings fluctuate relatively slightly, while that of the micro-structured coatings monotonously increase as the thermal shock temperature difference increases. (2) Apart from the difference in porosity of the coating, the interfacial bonding strength of micro-structured coating-substrate systems decreases as the temperature increases, while that of the nanostructured coating-substrate systems changes a little. Therefore, the bending strength of nanostructured coating-substrate systems fluctuates relatively slightly, while that of micro-structured coating-substrate systems monotonously increases as the thermal shock temperature difference increases. In conclusion, in the temperature range we studied, the mechanical properties of nanostructured coatings are less sensitive to the change of temperature and more stable than micro-structured coatings.

Acknowledgements

This work was supported by the National Basic Research Program of China (2012CB937500), the National Natural Science Foundation of China (10802088, 10832008, and 11023001), and the Opening Fund of LNM.

References

[1] P.F. Zhao, C.A. Sun, X.Y. Zhu, F.L. Shang, C.J. Li, Fracture toughness measurements of plasma-sprayed thermal barrier coatings using a modified four-point bending method, Surf. Coat. Technol., 204 (2010) 4066-4074.

[2] N.P. Padture, M. Gell, E.H. Jordan, Thermal barrier coatings for gas-turbine engine applications, Science, 296 (2002) 280-284.

[3] B. Liang, C. Ding, Thermal shock resistances of nanostructured and conventional zirconia coatings deposited by atmospheric plasma spraying, Surf. Coat. Technol., 197 (2005) 185-192.

[4] C. Zhang, C. Zhou, H. Peng, S. Gong, H. Xu, Influence of thermal shock on insulation effect of nano-multilayer thermal barrier coatings, Surf. Coat. Technol., 201 (2007) 6340-6344.

[5] Q.G. Fu, H.J. Li, Y.J. Wang, K.Z. Li, L. Wei, Influence of Thermal Shock on the Mechanical Behavior of Si-SiC Coated Carbon/Carbon Composites, J. Mater. Sci. Technol., 25 (2009) 251-253.

[6] G.-F. Peng, S.-H. Bian, Z.-Q. Guo, J. Zhao, X.-L. Peng, Y.-C. Jiang, Effect of thermal shock due to rapid cooling on residual mechanical properties of fiber concrete exposed to high temperatures, Constr. Build. Mater., 22 (2008) 948-955.

[7] C. Aksel, Mechanical properties and thermal shock behaviour of alumina–mullite–zirconia and alumina–mullite refractory materials by slip casting, Ceram. Int., 29 (2003) 311-316.

[8] F. Song, S. Meng, X. Xu, Y. Shao, Enhanced Thermal Shock Resistance of Ceramics through Biomimetically Inspired Nanofins, Phys. Rev. Lett., 104 (2010).

[9] G. Soyez, J.A. Eastman, L.J. Thompson, G.R. Bai, P.M. Baldo, A.W. McCormick, R.J. DiMelfi, A.A. Elmustafa, M.F. Tambwe, D.S. Stone, Grain-size-dependent thermal conductivity of nanocrystalline yttria-stabilized zirconia films grown by metal-organic chemical vapor deposition, Appl. Phys. Lett., 77 (2000) 1155-1157.

[10] J.-Y. Kwon, J.-H. Lee, Y.-G. Jung, U. Paik, Effect of bond coat nature and thickness on mechanical characteristic and contact damage of zirconia-based thermal barrier coatings, Surf.

Coat. Technol., 201 (2006) 3483-3490.
[11] J.A. Thompson, T.W. Clyne, The effect of heat treatment on the stiffness of zirconia top coats in plasma-sprayed TBCs, Acta Mater., 49 (2001) 1565-1575.
[12] R.M. Spriggs, Expression for Effect of Porosity on Elastic Modulus of Polycrystalline Refractory Materials, Particularly Aluminum Oxide, J. Am. Ceram. Soc., 44 (1961) 628-629.
[13] H. Deng, H. Shi, S. Tsuruoka, Influence of coating thickness and temperature on mechanical properties of steel deposited with Co-based alloy hardfacing coating, Surf. Coat. Technol., 204 (2010) 3927-3934.
[14] Z.B. Chen, Z.G. Wang, S.J. Zhu, Tensile fracture behavior of thermal barrier coatings on superalloy, Surf. Coat. Technol., 205 (2011) 3931-3938.
[15] N. Zotov, M. Bartsch, G. Eggeler, Thermal barrier coating systems — analysis of nanoindentation curves, Surf. Coat. Technol., 203 (2009) 2064-2072.
[16] L.Z. He, Q. Zheng, X.F. Sun, G.C. Hou, H.R. Guan, Z.Q. Hu, Low ductility at intermediate temperature of Ni–base superalloy M963, Mater. Sci. Eng., A, 380 (2004) 340-348.
[17] D. W., Discussion of Ryshkewitch paper, J. Am. Ceram. Soc., 36 (1953) 68.